

Update on the search for non fermionic neutral Higgs couplings at LEP 2

S. Andringa¹, P. Gonçalves¹, A. Onofre¹,
R. Paiva¹, L. Peralta¹, M. Pimenta¹ and B. Tomé¹

¹ LIP-IST-FCUL, Av. Elias Garcia, 14, 1, P-1000 Lisboa, Portugal

Abstract

Final states with isolated photons were explored in order to search for Higgs bosons with non fermionic couplings. The data collected by the DELPHI detector at centre-of-mass energies ranging from 192 GeV to 202 GeV corresponding to a total integrated luminosity of 230 pb⁻¹ were analysed. No evidence for a signal was found and confidence limits were derived in the framework of possible extensions of the SM Higgs sector.

1 Introduction

This note updates the search for the Higgs boson in events with isolated photons in DELPHI reported in [1, 2]. The analyses follow closely the previous ones and therefore the main focus is given to the obtained new results. The data were taken at centre-of-mass energies of 192 GeV, 196 GeV, 200 GeV and 202 GeV corresponding to integrated luminosities of 26 pb⁻¹, 77 pb⁻¹, 85 pb⁻¹ and 42pb⁻¹, respectively.

In the Standard Model (SM) Higgs couplings to photons are severely suppressed, however, in several of its extensions these couplings become important and can constitute a rather distinctive signature. Non fermionic couplings are studied in this note in two different frameworks. In one of them the SM Lagrangian is extended by introducing anomalous couplings of the Higgs boson to the vector bosons which lead in particular to direct H $\gamma\gamma$ and HZ γ couplings [3]. In the second framework a Higgs sector with two doublets is considered, in the particular case of the fermiophobic scenario [4]. Limits on $\sigma(e^+e^- \rightarrow Hq\bar{q}) \times \text{BR}(H \rightarrow \gamma\gamma)$ from another LEP experiment can be found in reference [5].

Anomalous Higgs couplings to the vector bosons can be expressed in terms of effective energy-dimension-six operators included in the interaction Lagrangian density [3]:

$$\mathcal{L}_{eff} = \sum_{i=1}^N \frac{f_i}{\Lambda^2} O_i, \quad (1)$$

where the O_i are the operators which represent the anomalous couplings, Λ is the typical energy scale of the interaction and f_i are the constants which define the strength of each term. Six operators give rise to the anomalous couplings H $\gamma\gamma$, HZ γ , HZZ and HWW, but only four, f_B , f_W , f_{BB} and f_{WW} , will be considered in what follows. The other two operators are bound by precise measurements of SM parameters. In this framework the Higgs boson can be produced at LEP in association with a Z or a γ . Signal events corresponding to Higgs boson masses (m_H) ranging from 80 to 195 GeV/c² were simulated using the PYTHIA generator [6]. The CompHEP package [7] was used for the computation of the cross-sections as a function of the anomalous couplings, f_i/Λ^2 , and of m_H .

The two Higgs Doublet Models (2HDM) without explicit CP violation [4] are characterised by five physical Higgs bosons: two neutral CP-even bosons (h^0 , H^0), two charged bosons (H^\pm), and one neutral CP-odd boson (A^0). The free parameters are usually chosen as the four Higgs masses and the angles α and β , where $\tan \beta$ represents the ratio of the vacuum expectation values of the two Higgs doublets and α the mixing angle of the neutral CP-even Higgs sector. In this paper only one of the Higgs doublet is allowed to couple to fermions (type I model [8]). The coupling of the lightest CP-even neutral boson h to a fermion pair is then proportional to $\cos \alpha$. If $\alpha = \frac{\pi}{2}$ this coupling vanishes and h becomes a fermiophobic neutral Higgs. The main mechanisms for the production of neutral Higgs bosons are $e^+e^- \rightarrow hZ^*$ and $e^+e^- \rightarrow hA$. These processes have complementary cross-sections, proportional to $\sin^2\delta$ and to $\cos^2\delta$ respectively, where $\delta = \alpha - \beta$. The dominant decay modes for $m_h < m_Z$ in the considered fermiophobic limit are $h \rightarrow AA$ (tree level) if $m_h > 2m_A$ and $h \rightarrow \gamma\gamma$ (one-loop) otherwise [4]. Above the Zh threshold the decay $A \rightarrow Zh$ is dominant for all the interesting region of δ ($\delta < 0.5$). In this region of masses the sensitivity is low, the analysis was done for 189 GeV data only and is reported in [1]. Below the Zh threshold A decays mainly into a $b\bar{b}$ pair. It should be noted that in the region of very low δ values ($\delta < 10^{-3}$) and $m_A < m_Z + m_h$ the A total

width is very small and it can leave the detector before decaying . All the processes, but the associated hA production with $h \rightarrow AA$, are characterised by the presence of isolated and energetic photons.

2 Event selection and Results

The tables 1 and 2 summarise the studied processes, the final state topologies and the relevant mass regions in the anomalous couplings and 2HDM frameworks, respectively. In the case of the $b\bar{b}b\bar{b}b\bar{b}$ final state the analysis of reference [9] is used.

Process	Final State	Relevant mass region (GeV)
$e^+e^- \rightarrow H\gamma$	$\gamma\gamma\gamma$ $b\bar{b}\gamma$	$80 < m_H < 170$
$e^+e^- \rightarrow HZ$	$\gamma\gamma\nu\bar{\nu}$	$80 < m_H < 100$
$e^+e^- \rightarrow HZ/\gamma^*$	$\gamma\gamma q\bar{q}$	$80 < m_H < 170$

Table 1: Studied topologies in the framework of the anomalous couplings model.

Process	Final states	Relevant mass region (GeV)
$e^+e^- \rightarrow h^0A^0$	$\gamma\gamma A^0$ (long lived) $\gamma\gamma b\bar{b}$	$m_A < m_Z + m_h$ $m_h + m_A > 40$
$e^+e^- \rightarrow h^0A^0 \rightarrow A^0A^0A^0$	$b\bar{b}b\bar{b}b\bar{b}$	$m_h > 2m_A$
$e^+e^- \rightarrow h^0Z$	$\gamma\gamma\nu\bar{\nu}$ $\gamma\gamma q\bar{q}$	$10 < m_h < 100$

Table 2: Studied topologies in the framework of the 2HDM.

The event selection was performed in three stages. In the first level, very general selection criteria were applied and the events were classified according to the number of jets and of isolated photons. No isolated leptons were allowed in the event. In the second level, different selection criteria were applied to each topology. In final states involving b quarks a third level based on a b tagging algorithm [10] was performed. Details on each selection level are given in reference [1]. Only small adjustments were made with respect to the previous analysis.

The number of candidates at different selection levels for the relevant topologies and centre-of-mass energies are given in table 3. The numbers in brackets give the Standard Model expectations. In the different selection levels and topologies, fair agreement between data and MC expectations is found and therefore 95% CL can be set on the parameters of both models as a function of the Higgs bosons masses.

The efficiencies, including the trigger efficiency, were calculated for each final state topology according to the the specific process to be studied at several mass points covering the relevant parameter space. The values shown in the last column of table 3 are average values.

These results together with the ones obtained at centre-of-mass energy of 189 GeV [1] were combined using the method described in [11] in both of the frameworks considered.

Energy GeV	topology	selection level			(ϵ)
		1	2	3	(%)
192	$\gamma\gamma\gamma$	96 (117 \pm 1)	2 (3.64 \pm 0.04)		50
	$\gamma\gamma$	96 (117 \pm 1)	82 (96.2 \pm 0.9)	1 (0.6 \pm 0.1) (hZ)	60
				1 (0.8 \pm 0.1) (hA)	60
	$b\bar{b}\gamma$	440 (490 \pm 7)	77 (88 \pm 3)	38 (43 \pm 2)	53
	$q\bar{q}\gamma\gamma$	52 (55 \pm 2)	5 (9 \pm 1)		40
	$b\bar{b}\gamma\gamma$	52 (55 \pm 2)	5 (9 \pm 1)	1 (4.0 \pm 0.6)	36
196	$\gamma\gamma\gamma$	344 (343 \pm 3)	11 (10.7 \pm 0.1)		50
	$\gamma\gamma$	344 (343 \pm 3)	274 (286 \pm 3)	1 (1.7 \pm 0.3) (hZ)	60
				1 (2.3 \pm 0.3) (hA)	60
	$b\bar{b}\gamma$	1347 (1355 \pm 20)	160 (205 \pm 7)	72 (99 \pm 5)	53
	$q\bar{q}\gamma\gamma$	144 (144 \pm 6)	19 (25 \pm 2)		40
	$b\bar{b}\gamma\gamma$	144 (144 \pm 6)	19 (25 \pm 2)	8 (13.4 \pm 1.7)	36
200	$\gamma\gamma\gamma$	334 (352 \pm 4)	11 (11.2 \pm 0.1)		50
	$\gamma\gamma$	334 (352 \pm 4)	271 (288 \pm 3)	2 (1.8 \pm 0.3) (hZ)	60
				3 (2.1 \pm 0.3) (hA)	60
	$b\bar{b}\gamma$	1378 (1396 \pm 21)	192 (213 \pm 8)	88 (100 \pm 5)	53
	$q\bar{q}\gamma\gamma$	146 (141 \pm 6)	22 (19 \pm 2)		40
	$b\bar{b}\gamma\gamma$	146 (141 \pm 6)	22 (19 \pm 2)	10 (10.2 \pm 1.5)	36
202	$\gamma\gamma\gamma$	173 (170 \pm 2)	7 (5.37 \pm 0.05)		50
	$\gamma\gamma$	173 (170 \pm 2)	129 (137 \pm 1)	2 (0.9 \pm 0.2) (hZ)	60
				2 (1.0 \pm 0.2) (hA)	60
	$b\bar{b}\gamma$	654 (645 \pm 11)	100 (88 \pm 4)	47 (44 \pm 3)	53
	$q\bar{q}\gamma\gamma$	79 (66 \pm 3)	14 (9 \pm 1)		40
	$b\bar{b}\gamma\gamma$	79 (66 \pm 3)	14 (9 \pm 1)	3 (4.6 \pm 0.8)	36

Table 3: Number of events passing the sets of cuts corresponding to the selection levels described in the text for each topology and centre-of-mass energy. The number of events predicted by the SM simulation and their statistical errors are displayed within parentheses. The efficiencies (ϵ) shown in the last column are average values.

3 Limits on anomalous couplings

Limits on the anomalous couplings were set assuming different scenarios. First each f_i parameter was considered independently by setting all the others to zero (figure 1). In a second scenario all f_i were set to a common value F (figure 2). In the scenario where only f_B or f_W are different from zero (figures 1 (c) and 1 (d)), the relevant channel is $b\bar{b}\gamma$ which has an important background contribution from radiative returns to the Z^0 . The $b\bar{b}\gamma$ is produced via a Z exchange in the s-channel and therefore the cross-section decreases above the Z mass. Despite these low cross-sections some sensitivity is kept even above 130 GeV since the SM background is concentrated around the Z mass and the expected levels at high mass are low.

The horizontal lines in figure 1 (c) are the limits obtained on the anomalous TGC parameter $\Delta k_\gamma = \frac{m_W^2}{2} \frac{(f_B + f_W)}{\Lambda^2}$ by the direct measurements of WW production [12].

4 Limits on fermiophobic Higgs boson production

The 95 % CL limits in the plane $(m_h, \sin^2\delta)$, obtained directly from the Higgs-strahlung final states, using the $h \rightarrow \gamma\gamma$ branching ratios computed in [4] using Potential A, are shown in figure 3.

If $\sin^2\delta = 1$ a lower limit of $m_h = 98 \text{ GeV}/c^2$ is established. For small values of $\sin^2\delta$ the Higgs-strahlung cross-section vanishes but an exclusion region can be obtained from the hA associated production. Such 95 % CL exclusion regions are shown for two A masses.

The complementarity of hZ and hA production channels was explored in order to set the 95 % CL exclusion region in the plane (m_h, m_A) shown in figure 4. For each pair of values (m_h, m_A) an upper (lower) limit on δ was obtained combining all the results concerning hA (hZ) mode. Whenever the upper limit is higher than the lower limit the corresponding point in the plane is excluded. The dark region in the figure 4 corresponds to the decay modes $h \rightarrow \gamma\gamma$ and $A \rightarrow b\bar{b}$ or A long-lived and is valid for all δ values. The light region was taken from reference [9] and corresponds to $h \rightarrow AA$ and $A \rightarrow b\bar{b}$.

Acknowledgements

We would like to thank L.Brücher and R.Santos for very interesting and long discussions in exploring the 2HDM fermiophobic scenario.

We are greatly indebted to our technical collaborators, to the members of the CERN-SL Division for the excellent performance of the LEP collider, and to the funding agencies for their support in building and operating the DELPHI detector.

References

- [1] S. Andringa, M. Espírito Santo, P. Gonçalves, A. Onofre, R. Paiva, L. Peralta, M. Pimenta and B. Tomé, “Search for non fermionic neutral Higgs couplings at LEP 2”, DELPHI 99-72 CONF 259
- [2] DELPHI Coll., P. Abreu et al., Phys. Lett. **B458** (1999) 431
- [3] K. Hagiwara, R. Szalapski, D. Zeppenfeld, Phys. Lett. **B318** (1993) 155
- [4] A. Barroso, L. Brücher, R. Santos, Phys. Rev. **D60** (1999) 035005
L. Brücher, R. Santos, Eur.Phys.J.**C12** (2000) 87
- [5] OPAL Coll., G. Abbiendi et al., Phys. Lett. **B464** (1999) 311
- [6] T. Sjöstrand, Comp. Phys. Comm. **82** (1994) 74,
T. Sjöstrand, Pythia 5.7 and Jetset 7.4, CERN-TH/7112-93
- [7] E.E. Boos, M.N. Dubinin, V.A. Ilyin, A.E. Pukhov, V.I. Savrin, Preprint INP MSU 94-36/358 and SNUCTP 94-116 (1994); hep-ph/9503280,
P.A. Baikov et al., in Proc. X Workshop QFTHEP-95 (Zvenigorod, September 1995), ed. B. Levtchenko and V. Savrin (MSU, Moscow, 1996) p.101; hep-ph/9701412
- [8] A G Akeroyd, “Three-body decays of Higgs bosons at LEP2 and application to a hidden fermiophobic Higgs”, (1998) hep-ph/9806337
J.F. Gunion, H.E.Haber, G.L.Kane and S. Dawson, “The Higgs Hunter’s Guide” (Addison-Wesley, Reading 1990)
- [9] DELPHI Coll. “Search for Neutral Higgs Bosons in e^+e^- Collisions at $\sqrt{s}=188.7$ GeV”, DELPHI 99-86 CONF 273
- [10] G.Borisov, C.Mariotti, DELPHI 97-16 PHYS672; DELPHI coll., P.Abreu et al., Nucl. Inst. Method. **A378** (1996) 57.
- [11] A.L. Read, “Optimal statistical analysis of search results based on the likelihood ratio and its application to the search for the MSM Higgs boson at $\sqrt{s}=161$ and 172 GeV”, DELPHI 97-158 PHYS 737
- [12] T.J.V. Bowcock et al., “Measurement of Trilinear Gauge Boson Couplings in e^+e^- Collisions at 189 GeV”, DELPHI 99-63 CONF 250

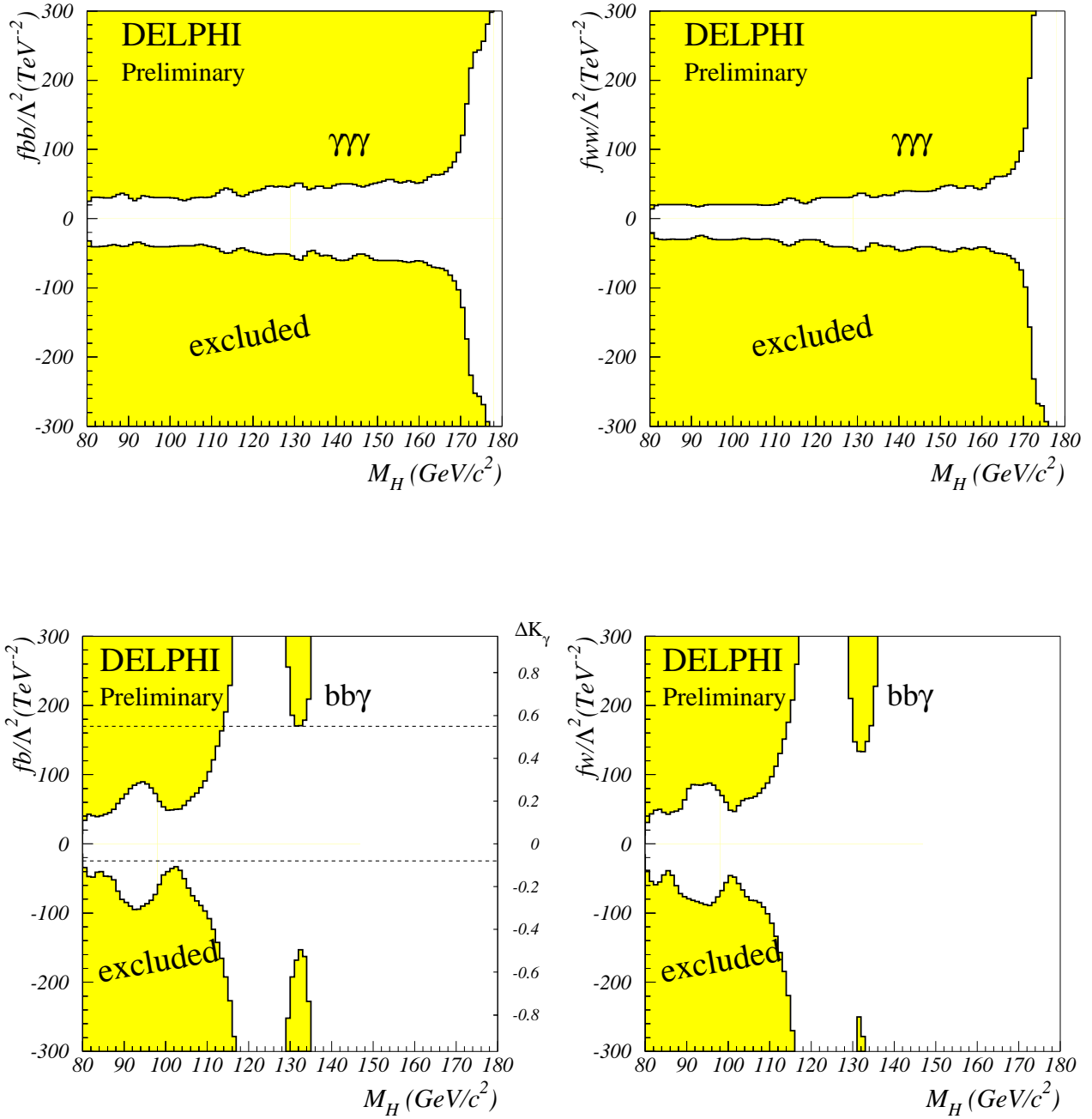


Figure 1: 95% CL limits on each f_i/Λ^2 parameter as a function of m_H , when all other f_i are set to zero. The exclusions correspond to the $\gamma\gamma\gamma$ analysis in (a) and (b) and $b\bar{b}\gamma$ analysis in (c) and (d). In c) the right hand scale corresponds to the TGC parameter Δk_γ . The data collected at centre-of-mass energies from 189 GeV to 202 GeV were used. The dashed line in c) is the 95% CL limit on Δk_γ from TGC measurements at 189 GeV.

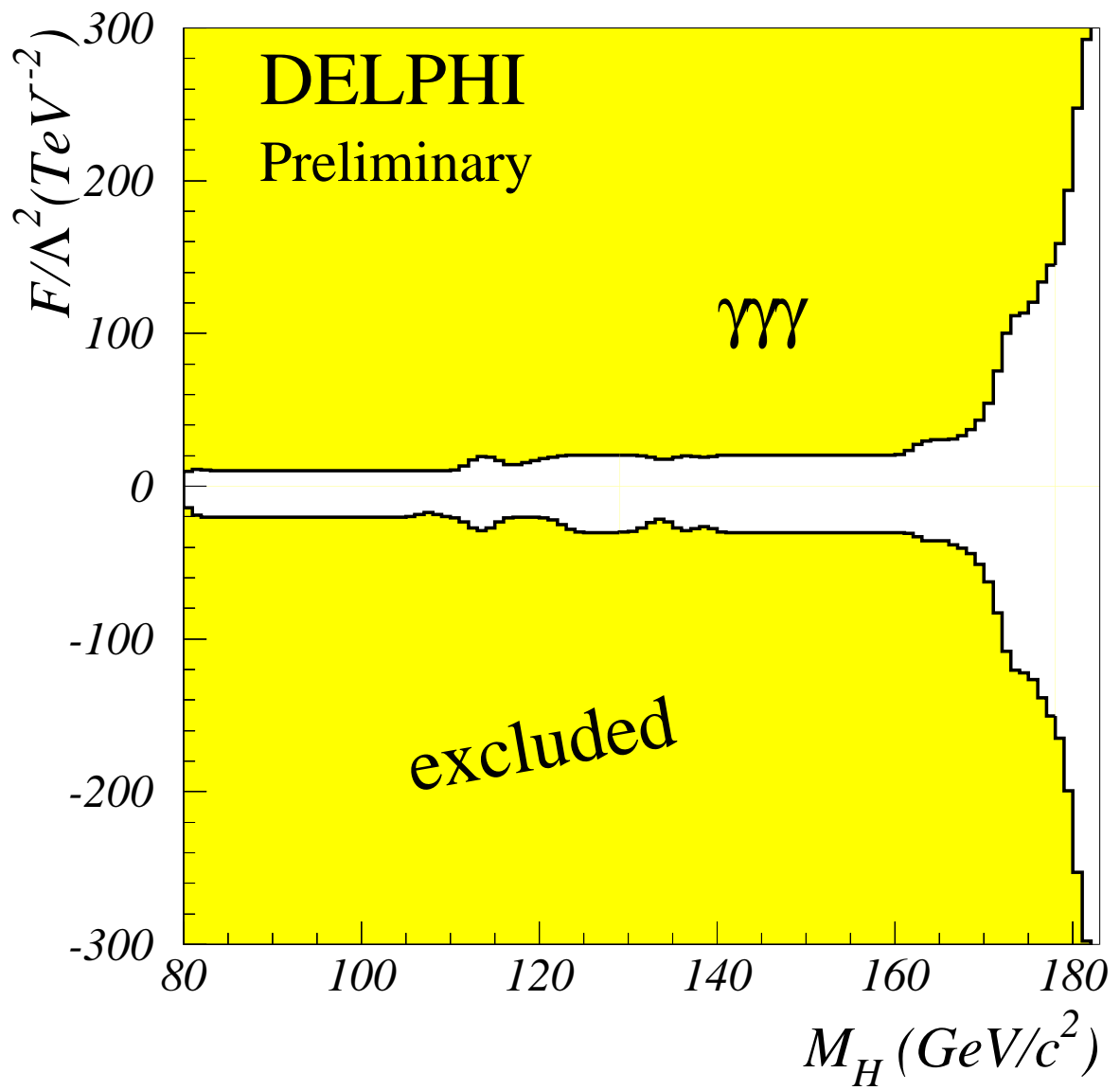


Figure 2: 95% CL limits on F/Λ^2 as a function of the Higgs boson mass. The exclusion is set by the $\gamma\gamma\gamma$ analysis in the data collected at centre-of-mass energies between 189 GeV and 202 GeV.

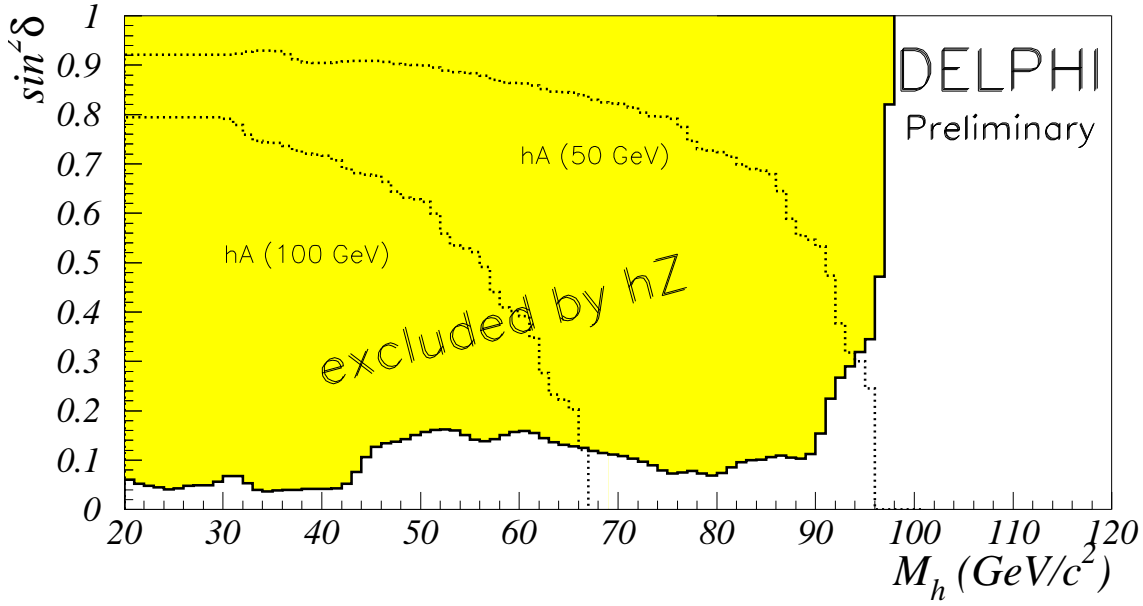


Figure 3: 95 % CL excluded region in the plane $(m_h, \sin^2\delta)$, obtained from the Higgs-strahlung final states. Also shown are the regions excluded by the associated process for $m_A = 50 \text{ GeV}/c^2$ and $m_A = 100 \text{ GeV}/c^2$. All the data at centre-of-mass energies between 189 GeV and 202 GeV were used.

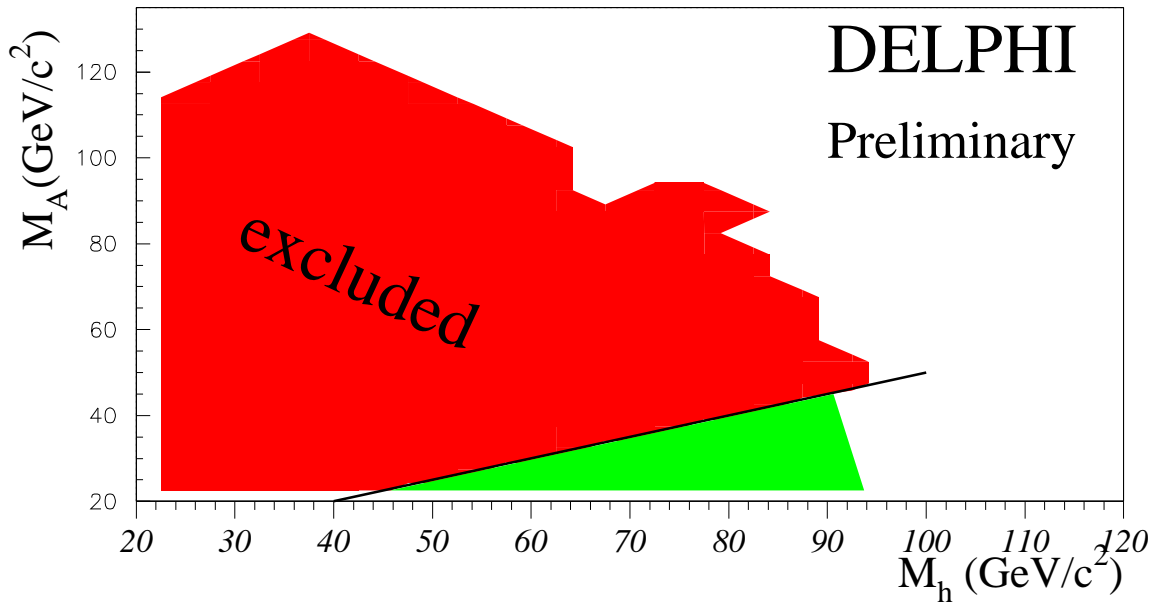


Figure 4: 95 % CL excluded region in the plane (m_h, m_A) , combining the Higgs-strahlung and the associated production process. The dark region corresponds to the decay modes $h \rightarrow \gamma\gamma$ and $A \rightarrow b\bar{b}$ or A long-lived, the limit is valid for all δ values. The analysis uses the data collected at centre-of-mass energies ranging from 189 GeV to 202 GeV. The light region was taken from reference [9] and corresponds to the analysis of $h \rightarrow AA$ and $A \rightarrow b\bar{b}$, for the data collected at a centre-of-mass energy of 189 GeV.